J. Appl. Res. Ind. Eng. Vol. 5, No. 2 (2018) 169–180

Journal of Applied Research on Industrial Engineering
www.journal-aprie.com

Experimental and CFD Analysis for the Solar Heat Pump by Using Phase Change Material

Saadoon Fahad Dakhil**, *Kifaya Oudah
Basra Engineering Technical College, Southern Technical University, Basra, Iraq.

PAPER INFO

Chronicle:
Received: 14 March 2018
Accepted: 28 August 2018

Keywords:
Free Convection.
Parafin Wax.
Heat Pump.
CFD.

ABSTRACT

The hot climate in Basra city requires many research to find a solution to reduce heat. Usually the thermal pump needs an external energy to ensure its continued operation. The objective of the study is the possibility of building a heat pump using renewable energy. The present work addresses a renewable energy heat bump by using paraffin wax during the daytime. The experimental and the CFD model of the solar collector and Thermal Energy Storage (TES) system based on Phase Change Materials (PCM) as a renewable heat pump system are presented. The system consists of three main parts: The solar collector, paraffin wax cavity, and cooling room. An experimental rig is constructed to conduct a practical analysis by measuring the intensity of solar radiation at different hours of the daytime. Temperatures distribution are measured with 24 type K thermocouples at different sites for the system. A numerical investigation has carried out to predict flow and heat transfer for the solar heat pump. Free convection of turbulent flow with 2-D unsteady state incompressible flow is examined. The numerical work is divided into two parts: The first part presents the development of numerical models of the heating collector room while the second is the numerical model of paraffin wax room. ANSYS FLUENT code 16 is applied to solve Navier Stock, energy, and k-Ɛ model equations by using finite volume method. The calculations of the velocity, temperatures distribution, and the Nusselt number values with different Rayleigh number for air at both heat collector room and paraffin wax room at different daytime are reported. The results of the present work guarantee future development of this technology for the food or agriculture industry. Maximum cooling temperature of the hot air is reached more than 20°C. It is found that a PCM leads to maximum energy savings and greater peak load at high solar intensity value. The practical results are also compared with numerical results, and good agreement is obtained.

1. Introduction

In the past years, more systems combining solar thermal collectors with heat pumps have been developed and introduced to the market for both domestic hot water and space heating. Usually, the thermal pump needs an external energy to ensure its continued operation. Now, renewable technologies are considered as clean sources of energy, and optimal use of these resource minimizes the environmental impacts, produces minimum secondary wastes and is sustainable based on current and future economic and societal needs. Clean energy generation becomes more and more crucial day by

* Corresponding author
E-mail address: s.albahadili@stu.edu.iq
DOI: 10.22105/jarie.2018.69846

day due to the growing significance of environmental issues. Renewable Energy Sources (RES) supply 14% of the total world energy demand. Renewable energy resources will play an important role in the world's future and are also often called alternative sources of classic energy. RES include biomass, hydropower, geothermal, solar, wind, and marine energies. Among the clean energy technologies, the solar energy is recognized as one of the most promising choices since it is free and provides clean and environmentally friendly energy [1]. Solar energy is available only during the day, and hence, its application requires an efficient thermal energy storage so that the excess heat collected during sunshine hours may be stored for later use during the night. Because of this limitation, researchers are required to treat this problem. This study aims at finding a solution to substitute for this weakness by using the phase change material for storing the energy during the time of the availability of solar energy.

A thermal solar collector is a device which absorbs the incoming solar radiation, converts it into heat, and transfers this heat to fluid (usually air, water or oil) flowing through the collector. Solar collectors are usually classified into two categories according to concentration ratios: Non-concentrating collectors and concentrating collectors. The non-concentrating has area of absorbing equal to the area exposed to the solar radiation, while in the state of concentrating, the solar collector has concave and reflexive surface to intercept and focus the beam of sun radiation and give it to a small area of reception [2].

Phase change materials process the ability to change their state with a certain temperature range. These materials absorb energy during the heating process as phase change that take place and release energy to the environment in the phase change range during a reverse cooling process. Materials to be used for phase change thermal energy storage must have a large latent heat and should have a melting temperature lying in the practical range of operation. Materials that have been studied during the last 40 years are hydrated salts, paraffin waxes, fatty acids and eutectics of organic and non-organic compounds. Depending on the applications, the PCMs should first be selected based on their melting temperature. Materials that melt below 15 ℃ are used for storing coolness in air conditioning applications, while materials that melt above 90 ℃ are used for absorption refrigeration. All other materials that melt between these two temperatures can be applied in solar heating and for heat load levelling applications.

Thermal Energy Storage (TES) is a promising technology to attenuate energy crunch and environmental problems. The storage of thermal energy is very important to many engineering applications [3]. Thermal Energy Storage (TES) can take the form of Sensible Heat Storage (SHS) or Latent Heat Storage (LHS). The Latent Heat Thermal Energy Storage (LHTES) method that is suitable for solar heating and air conditioning, can store much more thermal energy for a given volume. When LHS is used to store solar energy, it can increase the thermal storage efficiency. PCMs are latent heat thermal storage materials [4]. Zhang and Faghri [5] studied a numerical solution of laminar forced convection heat transfer of a microencapsulated phase change material suspension in a circular tube with constant heat flux. Lamberg and sire [6] studied the analytical model based on a quasi-linear, transient, thin-fin equation for melting in a semi-infinite PCM storage with an internal fin. Heim [7] studied a comparative two solution methods of specific and latent heat transfer in building components, e.g. walls, ceilings or floors numerically. This study is a contribution to the integration of latent heat storage materials to the integration of latent heat storage materials with the whole building dynamic simulation using two different approaches. Carbonari et al. [8] studied numerically and experimental analyses of PCM containing sandwich panels for prefabricated walls. A finite element numerical algorithm used for the simulation of two dimensional problems of heat transfer with phase change is veracious. Four prototypes of PCM containing sandwich panels for prefabricated walls were tested (two of them

validate the numerical finite element method for design purposes) in a test-room capable of simulating several kinds of outdoor and indoor environmental conditions; comparing the numerical results with the experimental ones derived from tests carried out on two different kinds of PCM containing sandwich panels.
Heat pump is a device which pumps heat from one or more low temperature sources to one or more high temperature sinks. Heat pumps are designed to move thermal energy opposite to the direction of spontaneous heat flow by absorbing heat from a cold space and releasing it to a warmer one [9]. Heat pumps are very efficient for heating and cooling systems, and can significantly reduce the energy costs. Until now there is no researchers interested in solar energy with PCM into the thermal applications. The aim of this study is to benefit from the changing material phase to build a thermal pump using renewable energy through combine the benefit of both solar energy as heat source and PCM material as a sustainable heat sink.

2. Theoretical Analysis

This section describes governing equations and numerical solutions by using Computational Fluid Dynamics (CFD) and description of the turbulence models k-Ɛ and boundary condition which are used in this study. Theoretical analysis includes two main parts only: Solar collector as the source heating room with inclined finned black wall. All fins are rectangular unformed cross section and fixed at equal interval space; Paraffin wax room as sink of absorb heat.

For system above, the heat conduction and free convection were analysed into two dimensional at turbulent flow with different solar intensity and daytime. To solve this problem, the following assumptions are necessary:

- Solar intensity fall on the solar collector as constant heat flux at a fixed time.
- The thermophysical properties of the PCM, solid and HTF (air) are independent of temperature.
- The PCM is homogeneous and isotropic.
- The PCM is initially in solid phase at initial temperature lower than melting temperature.
- The heat transfer in the PCM is controlled only by conduction.
- The flow of HTF is two dimensional, incompressible, turbulent flow, no slip, and steady state velocities with variable temperature with time.
- The energy dissipation of HTF is negligible.
- The pressure gradient of HTF flow is in axial direction only.

Now, based on the previous assumption, the system of equations governs the velocity, and the temperature fields of HTF are written as follows [9]:

Continuity equation

$$\frac{\partial u}{\partial x}+\frac{\partial v}{\partial y}=0. \qquad (1)$$

X-momentum equation

$$u\frac{\partial u}{\partial x}+v\frac{\partial u}{\partial y}=-\frac{1}{\rho_f}\frac{dp}{dx}+\frac{\mu_f}{\rho_f}\left(\frac{\partial^2 u}{\partial x^2}+\frac{\partial^2 u}{\partial y^2}\right). \qquad (2)$$

Y-momentum equation

$$u\frac{\partial u}{\partial x}+v\frac{\partial u}{\partial y}=\frac{\mu_f}{\rho_f}\left(\frac{\partial^2 u}{\partial x^2}+\frac{\partial^2 u}{\partial y^2}\right). \tag{3}$$

Energy equation

$$\frac{\partial T_f}{\partial t}+u\frac{\partial T_f}{\partial x}+v\frac{\partial T_f}{\partial y}=\frac{k_f}{c_f}\left(\frac{\partial^2 T_f}{\partial x^2}+\frac{\partial^2 T_f}{\partial y^2}\right). \tag{4}$$

Also, the suitable and simplified governing energy equation for two dimensional and unsteady state heat transfer in the solid paraffin without heat generation is shown below:

$$\frac{\partial T_s}{\partial t}=\frac{k_s}{c_s}\left(\frac{\partial^2 T_s}{\partial x^2}+\frac{\partial^2 T_s}{\partial y^2}\right). \tag{5}$$

By solving the governing equations, the discretization equations for the velocity, pressure, and temperature fields can be obtained. The governing equations are solved numerically using the finite volume method (Upwind scheme) by explicit difference for time and forward difference [10]. All discretization equations except energy equations are solved by using the SIMPLE (Semi-Implicit Method for Pressure–Linked Equations) algorithm method. Numerical model was employed for complete results which was solved with help of ANSYS FLUENT code 16.0. From the obtained pressure, velocity, and temperature distributions, respectively, one can determine the axial variation of the thermal performance as average Nusselt number.

3. Initial and Boundary Conditions

- Initial condition: T=0 at time=0.
- The solar collector; collector is inclined finned wall: Constant heat flux and no slip wall: u=v-0. All fins are insulated at tip t> 0.
- All Inlet and outlet pipes are insulated.
- Paraffin room: Walls are insulated and no slip condition; paraffin top surface is coupling boundary; fluid-solid interfaces at t>0**.**

$$\left.\begin{aligned} &u=v=0\\ &-k_f\frac{\partial T_f}{\partial y}=-k_p\frac{\partial T_p}{\partial y}\end{aligned}\right\}$$

Paraffin bottom surface is coupling boundary and solid-fluid interfaces at t>0.

$$\left.\begin{aligned} &u=v=0\\ &-k_f\frac{\partial T_f}{\partial y}=-k_p\frac{\partial T_p}{\partial y}\end{aligned}\right\}$$

Thermo-physical properties of tested paraffin wax are as follows [10]:

Parameters	Values
Density [kg/m3]	880 (solid)/760 (liquid)
Specific heat [kJ/kg K]	2.9 (solid)/2.2 (liquid)
Thermal conductivity [W/m K]	0.2
Melting temperature [^{o}C]	51
Latent heat [kJ/kg]	140
Thermal expansion [K-1]	0.001

4. Experiment Setup

Photograph of the experimental setup with the solar collector connected to the PCM room is shown in Fig. 1. The setup consists of an insulated room which holds 25 kg PCM layer and inclined solar finned flat plate collector. The cork box has a capacity of about (0.79 * 0.43 * 0.5) mm filled with paraffin wax and fixed above the collector room. The solid PCM is encapsulated in the cork room, height of 100 mm. The collector room consist of inclined black finned wall fixed at the top face of the cork room with an internal length of (790) mm and a height of (860) mm. It houses in the PCM room with insulated pipe dia (100) mm and allows hot air to flow over the PCM layer, then heat transfer between the PCM and the air is occurred. All pipes and rooms are insulated with 50 mm of glass wool. At 150 cm bottom side, the cooling room is placed and the closed circular system is constructed. The thermocouples are the type K and are fixed at 24 different sites as follow: 9 at collector room, 9 at paraffin room, and others at inlet and outlet ports of each pipe. All thermocouples are fixed to H112 heat transfer service unit as selector for reading temperature. A pyrometer is used to measure total hemispherical radiation-beam plus diffuse on a horizontal and inclined surfaces. The type of action meter is used for measuring solar irradiance and the solar radiation flux density (w/m^2) from the hemisphere within a wavelength range o.3 μm to 3 μm.

Fig. 1. *Photgraph view of solar heat pump with PCM.*

1) Storage plate, 2) Thermocouple "K", 3) Solar collector, 4) Pipe, 5) H112 Heat transfer service unite (HTSU), 6) Paraffin room, 7) Insulato), 8)Cooling room.

5. Results and Discussion

This section presents the results obtained from the theoretical and experimental works. The first part of the analysis is a convergence study for the proposed numerical code. The second part presents the experimentally results from the measured data. Then, the final is the comparisons between numerical and experimental results.

Fig. 2 presents the numerical results of the air stream function through the heat pump at Ra=15x10^{11}. The effect of free convection is clearly appeared along the system. The variation of stream function means that there is a change in power between the intensity of radiation as a source of heat absorbed by PCM. Also Fig. 3 shows the same contour but for velocity magnitude of air inside heat pump. The maximum velocity is reached about 0.17 m/s through the inlet port of the paraffin room.

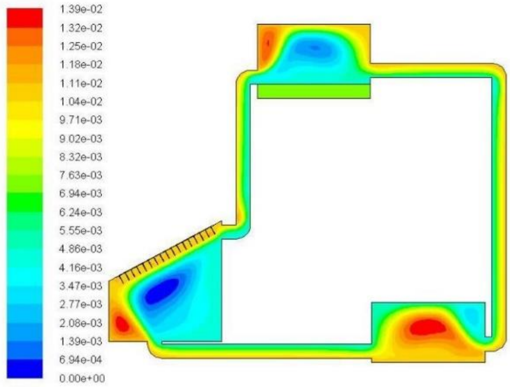

Fig. 2. *Coture of stream function for system during 21 May 2018 and Ra=15x10^{11}.*

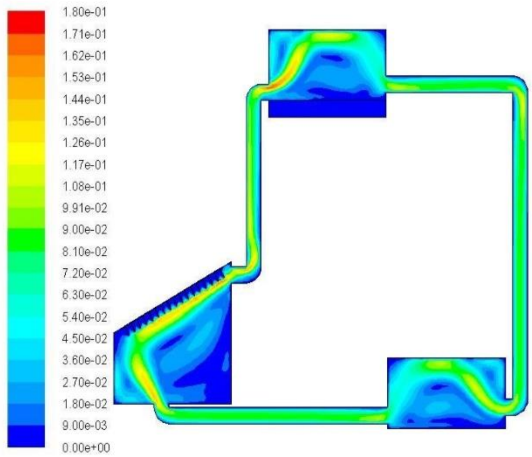

Fig. 3. *Coture of velocity magnitude for system during 21 May 2018 and Ra=15x10^{11}.*

Fig. 4 shows the thermal numerical results for the inclined finned wall with time. Results present the temperature distribution along the wall through one hour with 10 min step. Highest values for temperature are recorded at time 12.0 AM. Theoretical prediction for solar intensity with different day in March 2018 at the climate of Basra city is presented at Fig. 5. In all days, the highest solar intensity is recorded at 12 hours and the maximum value at BASRAH during March is reached to 900 w/m^2. From the energy equation and the numerical solution, the average Nusselt number is presented at Figure 6 with different inclination angle of the collector wall. At constant heat flux, the high Nusselt number means low temperature difference, so, at angle Ø =30º, the value of Nu_{avg} lower than angle 28º. At initial value, the maximum Nu_{avg} is occurred, then decreased at the end time. Experimentally at the climate of Basra city the sun radiation is 30º.

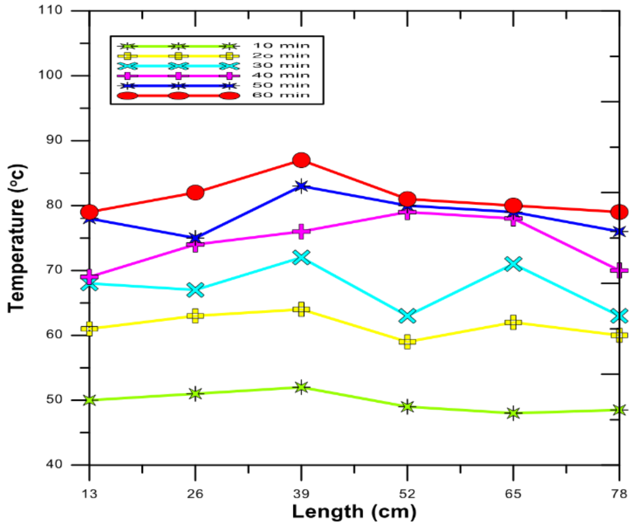

Fig. 4. *Variation temperature along the collector wall with time at Ø=30º and Ra=14*10^{11}, (15 March, 11.0→12.0 AM) (CFD).*

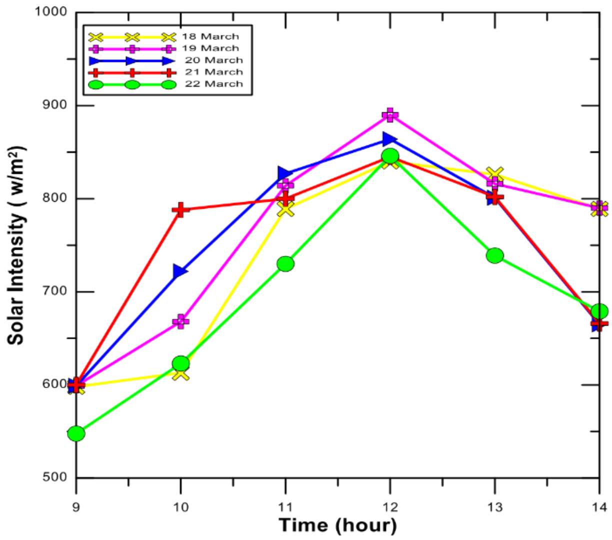

Fig. 5. *Solar intensity variation at different day with time at Ø=30º (March 2018) (CFD).*

Experimentally, the temperature distribution is recorded along the collector wall at Ø=30º and Ra=14*10^{11} with different time along one hour. The high level of the temperatures are indicated at hour 13.0 PM as shown in Fig. 7.

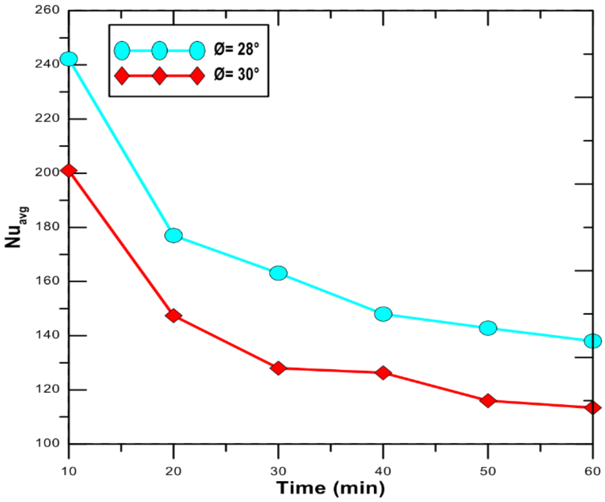

Fig. 6. *Nu$_{avg}$ of air inside solar collector with different Ø and Ra=15*10^{11} (15 May, 11.0→12.0 AM) (CFD).*

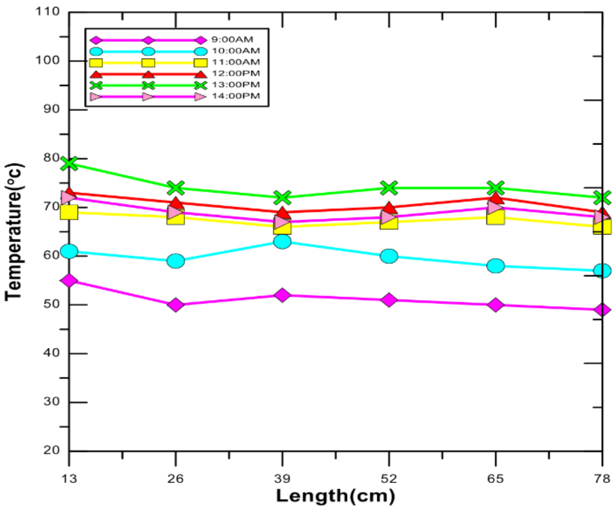

Fig. 7. *Variation temperatures along the collector plate at Ø=30º and Ra=14*10^{11} (15 March) (Exp).*

Thermal analysis of paraffin room is examined experimentally as is explained in Fig. 8 at 10 Min interval time. Temperatures distribution along the paraffin wall at Ø=30º melting point 53ºC and Ra=14*10^{11} are recorded. For all times, the paraffin wall temperature is decreased with the increased length due to the heat transfer between hot air and solid paraffin.

Fig. 9 shows the variation of the Nu_{avg} of paraffin at Ø=30º, Ra=15*10^{11}, and melting point 53ºC during 15 March with interval time equal to 10 Min.

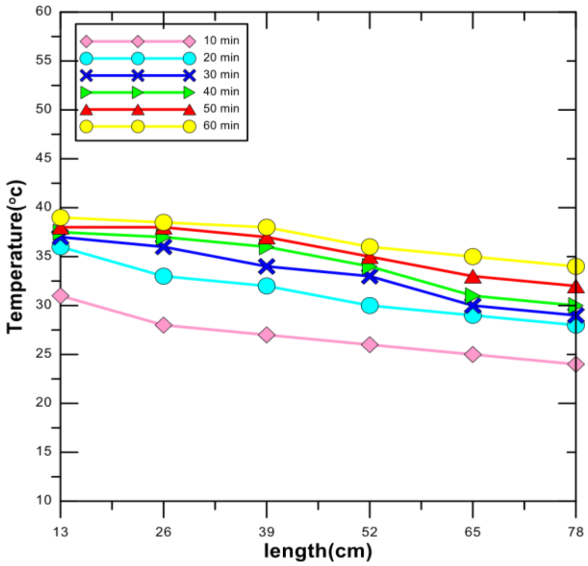

Fig. 8. *Variation temperature along the paraffin wall at Ø=30º, melting point 53ºC, and Ra=14*10^{11} (15 March, 11→12 AM) (Exp).*

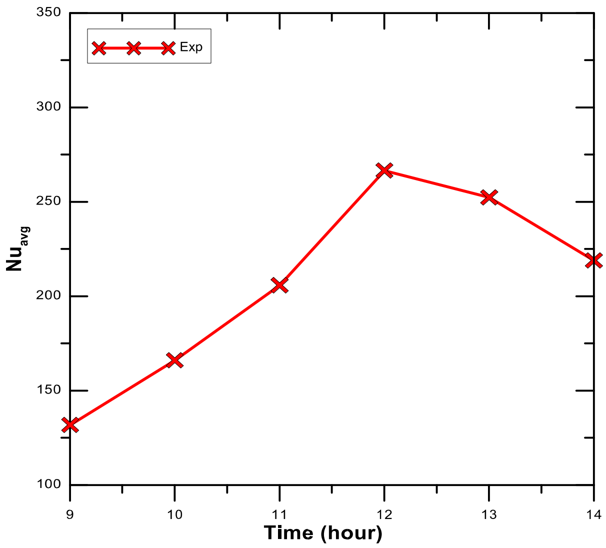

Fig. 9. *Nu_{avg} of paraffin at Ø=30º, Ra=15*10^{11}, and melting point 53ºC (15March) (Exp).*

Fig. 10 presents the comparison of the paraffin wall temperature at Ø =30º, Ra=15*10^{11}, and melting point 53ºC (15 May, 11→12 AM). The results show an increase of the average wall temperature when time increases due to charging energy by PCM. Also, it illustrates a good agreement between theoretical and experimental results. The average temperatures for collector wall are explained at Fig. 11 during months March and May, respectively. Also the average wall temperature is increased with time as explained in Fig. 7. The comparison shows good agreement at all times. Finally, the important result is presented in Fig. 12. Results show good performance for the heat pump by using PCM together with solar energy and the difference between the hot air exit from the collector and the cold air exit from the cooling room more than 20ºC at the climate of Basra city, furthermore, the good agreement between CFD and experimental results.

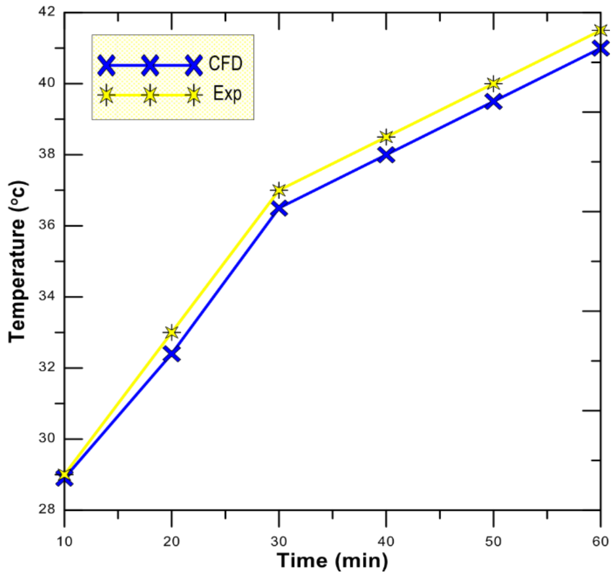

Fig. 10. *Comparison of the paraffin wall temperature at Ø =30º, Ra=15*10¹¹, and melting point 53ºC (15 May, 11→12 AM).*

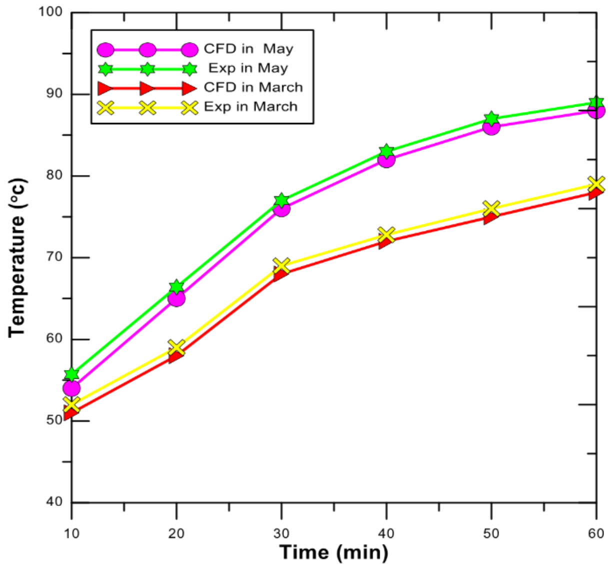

Fig. 11. *Comparison of the collector wall temperature at Ø =30º, Ra=14*10¹¹, and Ra=15*10¹¹, respectively 11.0→12.0 AM.*

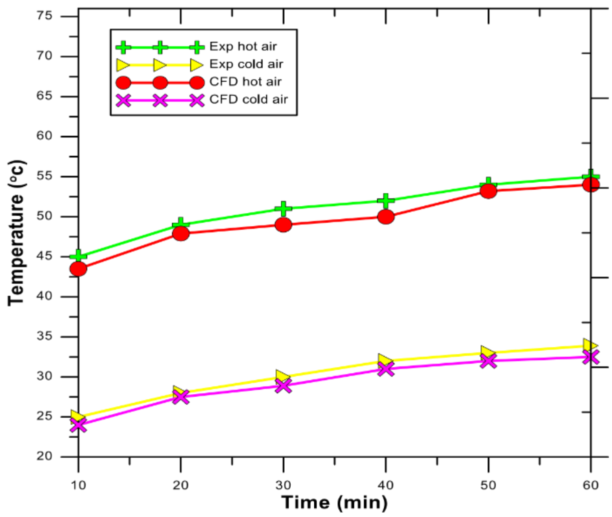

Fig. 12. *Comparison of the temperatures for hot air exit and cold air exit in March at Ø=30º, Ra=14*10¹¹, and 11.0→12.0 AM.*

6. Conclusion

Energy storage plays an important roles in conserving available energy and improving the solar energy applications. This work was based on two parts: The first part focused the development of numerical models for simulating the transient behaviour of the solar PCM energy to predict the energy balance in space, time, and the overall performance and their application to several test cases; the second part described the design and the implementation of a test rig that specifically built for the experimental investigation of heat storage devices. The renewable heat pump is used in many fields such as protected agriculture, poultry fields, and birds that needs the large cooling areas. This work will be the beginning of the development of incubators and protected areas that require special climatic conditions.

Nomenclature

ρ	Density	k	Turbulent energy
β	Thermal expansion	Ɛ	Turbulant disspation energy
T_m	Melting temperature	u,v	Fluid velocity
T_p	PCM temperature	Ø	Collector inclination angle
T_f	Fluid temperature	CFD	Computation fluid dynamics
PCM	Phase change material	*C*	Specific heat
T_s	Solid temperature	*k*	Thermal conductivity
g	Gravity	*μ*	Dynamic viscosity
t	Time	*Exp*	Experiment

References

[1] Veremachi, A., Cuamba, B. C., Zia, A., Lovseth, J., & Nydal, O. J. (2016). PCM heat storage charged with a double-reflector solar system. *Journal of solar energy.* doi: http://dx.doi.org/10.1155/2016/9075349

[2] Fokaides, P. A., Kylili, A., & Kalogirou, S. A. (2015). Phase change materials (PCMs) integrated into transparent building elements: a review. *Materials for renewable and sustainable energy*, *4*(2), 6.

[3] Tan, L., Kwok, Y., Date, A., & Akbarzadeh, A. (2012). Numerical study of natural convection effects in latent heat storage using aluminum fins and spiral fillers. *International journal of mechanical and aerospace engineering*, *6*, 238-245.

[4] Brousseau, P., & Lacroix, M. (1996). Study of the thermal performance of a multi-layer PCM storage unit. *Energy conversion and management*, *37*(5), 599-609.

[5] Zhang, Y., & Faghri, A. (1995). Analysis of forced convection heat transfer in microencapsulated phase change material suspensions. *Journal of thermophysics and heat transfer*, *9*(4), 727-732.

[6] Lamberg, P., & Siren, K. (2003). Analytical model for melting in a semi-infinite PCM storage with an internal fin. *Heat and mass transfer*, *39*(2), 167-176.

[7] Heim, D. (2005, August). Two solution methods of heat transfer with phase change within whole building dynamic simulation. *9th international IBPSA conference (pp. 397-402).* Montréal, Canada.

[8] Carbonari, A., De Grassi, M., Di Perna, C., & Principi, P. (2006). Numerical and experimental analyses of PCM containing sandwich panels for prefabricated walls. *Energy and buildings*, *38*(5), 472-483.

[9] Spence, E. (2010). *Characterization of the operational efficiency of a domestic heat pump* (Master's thesis, University of Strathclyde Engineering). Retrieved from http://www.esru.strath.ac.uk/Documents/MSc_2010/Spence.pdf

[10] Fluent, A. (2009). *12.0 User's guide*. Ansys Inc.